HARDENING MODEL OF ALUMINUM-BASED ALLOYS AFTER CONVENTIONAL PLASTIC DEFORMATION

[1]Fadi ABOUHILOU, [1]Lynda ABBANE, [2]Mohammed ATMA

[1]USTHB, Faculty of Physics, Department of Materials Physics, Materials Physics Laboratory, El alia, BP 32 Bab-Ezzouar, Algeria, abouhiloufadi@gmail.com, abbanelynda16@gmail.com

[2]Ferhat Abbas Sétif-1 University, Faculty of Sciences, Physics Department, Laboratory of Dosing, Analysis and Characterization with High Resolution (DAC-hr), Setif, Algeria, atmamohamed@gmail.com

https://doi.org/10.37904/metal.2022.4501

Abstract

The main objective is to model the plastic behavior of the three aluminum alloys 1050, 2024 and 7075.In the first part, using the experimental results of uniaxial tensile tests for each alloy and in the three main directions, and using a strategy of identifying the parameters of each work hardening model studied, Hollomon, Swift and Voce, we have created an empirical database of 1050, 2024 and 7075 aluminum series alloys.In the second part, one established the curves of uniaxial tensile curve by using the work hardening laws and the experimental parameters obtained in the first part. The comparison with the experimental data shows that the plastic behavior model can successfully describe with the use of appropriate workhardening law for each alloy.

Keywords: Lankford, work hardening models, aluminum alloys, anisotropy, tensile tests

1. INTRODUCTION

Aluminum alloy is a chemical composition where other elements are added to pure aluminum in order to improve its properties. These elements include iron, silicon, copper, magnesium, manganese and zinc in combined concentrations of up to 15% of the alloy by weight [1].

The 1XXX series alloys are made of 99% or greater pure aluminum. This series has excellent corrosion resistance, excellent workability, as well as high thermal and electrical conductivity [2]. Common alloys in this series are 1100 for electrical conductors and decorative items, 1050 for heat exchangers and pans and 1350, for electrical applications [3-4]

Alloys of the 2XXX series contain, as additives, beside copper (up to 6 wt%), also magnesium, silicon and manganese (up to 1-2 wt%) as well as small amounts of iron, nickel, titanium, zirconium and lithium. They characterize in good mechanical properties and they have the properties of heat-resisting materials, owing to the formation of phases rich in Fe, Mn and Ti [5-6].

Aluminum alloys 7075 falls into this category. It is one of the strongest aluminum alloys with high strength to weight ratio. Apart from the high strength, the alloy has particularly high response to natural age hardening which makes it a natural choice for a number of aircraft structural applications, military vehicles, earth moving equipment, bridges and other highly stressed defense applications [7-8]. Al 7075 alloy has zinc, magnesium and cooper as its major alloying elements. The alloy derives its strength from precipitation of $Mg2Zn$ and $Al2CuMg$ phases [6].

Aluminum alloys 2024, 7075 occupy a very important place in the aeronautical field. They have a low density, which is an asset for reducing the weight of aircraft. In addition, they have high characteristics. Indeed, seventy percent of the structure of a Boeing 777 is made of precipitation hardening alloys of the 2xxx and 7xxx series [9]. Among the alloys of these two series are alloys 2024 and 7075.

In this work, we were interested in 1XXXX (1050 for 99.5% of Al and 0.5% others), 2XXX (2024 for Al and Cu) and 7XXX (7075 for Al and Zn and Mg) series of aluminum which are widely used in aeronautics. They are produced in sheet form because they usually undergo shaping by conventional plastic deformation like hot or cold rolling and the modeling of the work hardening behavior of alloys based on aluminum using three models: Holomon, Swift and Voce hardening laws.

2. EXPERIMENTAL PROCEDURE

Three commercial alloys 7075, 2024 and 1050 in the form of sheets of thickness 2.0, 1.5 and 1.0 mm successively in the states received. A cutting of the samples of (4 cm in length and 4 cm in width) is carried out followed by a cutting of tensile test specimens in the three directions (0◦, 45◦, 90◦) with respect to the rolling direction as indicated in **Figure 1**. The dimensions of the flat tensile test specimen are shown in **Figure 2.** The tensile tests were carried out with an MTS MTSZ Roell type drill bit (CRTI) at an initial strain rate of 10^{-2} s^{-1} at room temperature.

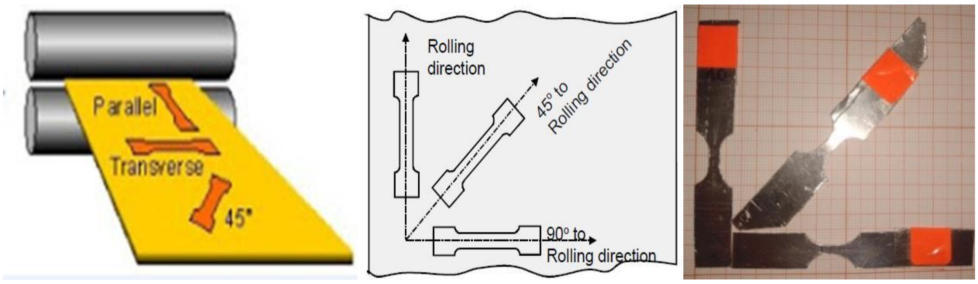

Figure 1 Sampling of specimens in the three directions with respect to the rolling direction.

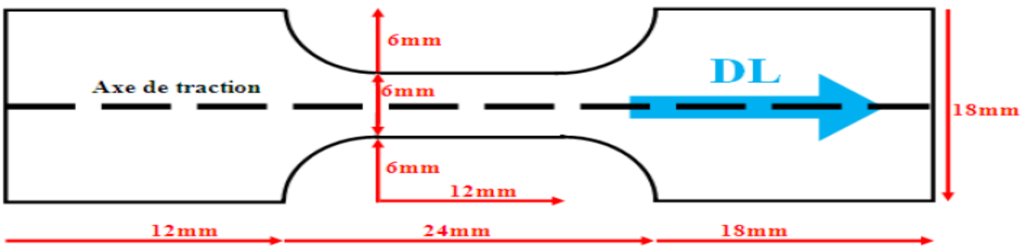

Figure 2 Representation of the dimensions of the tensile tests used in this study.

3. KINEMATIC HARDENING MODELS

3.1. Hollomon hardening law

One of the simplest laws is Hollomon hardening law, this law is based only on two parameters (K_H and n_H) does not provide any information on the elastic limit [10].

$$\sigma = K_H \varepsilon_p^{\ n_H} \qquad (1)$$

where: σ - the stress (MPa); ε_p- the plastic strain (-); K_H - the strength coefficient (MPa); n_H - strain-hardening exponent (-).

In the Hollomon hardening expression, the strain-hardening exponentmeasures the ability of a metal to strain-harden; largermagnitudes indicate larger degrees of strain hardening. Formost metals, the strain-hardening exponent falls between0.10-0.50.

3.2. Swift hardening law or Krupkowski hardening law:

In turn, Swift introduced the constant into the strain term, which is written [11]:

$$\varepsilon = \varepsilon_0 + K_S \sigma^{n_S} \quad \text{or} \tag{2}$$

$$\sigma = K'_S \left(\varepsilon_p + \varepsilon_0\right)^{n'_S} \tag{3}$$

where: ε_0, K_S, K'_S, n_S and n'_S are the parameters.

Note that with this law, the yield stress of the material is

$$\sigma_e = K'_S \varepsilon_p^{\ n'_S} \tag{4}$$

3.3. Voce hardening law:

In modeling the strain-hardening curve at elevated temperatures based on the relationship between stress and strain defined by Voce (1948) [12], the following function is used [13]:

$$\sigma = \sigma_1 + \left(\sigma_S - \sigma_1\right)\left[1 - \exp\left(-\frac{\varepsilon_p - \varepsilon_1}{\varepsilon_c}\right)\right], \tag{5}$$

where ε_p is a plastic strain, σ_1 and ε_1 represent first measurement of the stress and the strain respectively, σ_s saturation stress, ε_c strain constant. If $\varepsilon_1 = 0$ (limit of applicability of Hook's law or yield point), then:

$$\sigma = \sigma_S - K_V \exp(n_V \varepsilon_p) \tag{6}$$

where $n_V = -1/\varepsilon_c$

4. IDENTIFICATION OF MODEL PARAMETERS

First identification:

To identify Hollomon parameters K_H and n_H, we transform the curve into: $\ln(\sigma) = f(\ln(\varepsilon_p))$, which becomes linear.

$$\ln(\sigma) = n_H \ln(\varepsilon_p) + \ln(K_H). \tag{7}$$

The slope of this curve gives the strain-hardening exponent n_H.

$$n_H = \frac{dLn(\sigma)}{dLn(\varepsilon_p)}. \tag{8}$$

Second identification:

To identify Swift parameters K'_S et n'_S, we transform the curve into $\ln(\sigma) = f(\ln(\varepsilon_0+\varepsilon_p))$, which becomes linear.

$$\ln(\sigma) = n'_s [\ln(\varepsilon_0 + \varepsilon_p) + \ln(K'_s)]. \tag{9}$$

The slope of this curve gives the coefficient n'_S.

$$n'_S = \frac{dLn(\sigma)}{dLn(\varepsilon_0 + \varepsilon_p)}. \tag{10}$$

Third identification:

To identify voce parameters we Use origin6.0, by the fit exponential decay the first order.

5. RESULTS AND DISCUSIONS

The**Table 1** shows the parameters of each alloy in the 1050, 2024 and 7075 series corresponding to each work-hardening model studied (Hollomon, Swift and Voce hardening laws). These parameterswere obtained after analyzing the tensile curves using previous identification methods for the received states.

Table 1 The values of the parameters in the Hollomon, Swift and Voce equations

		Hollomon		Swift			Voce		
	α (°)	K_H(MPa)	n_H	K_H(MPa)	n_S	$\varepsilon 0$	σ_{sat}(MPa)	K_v(MPa)	n_v
1050	0	155.67959	0.21848	208.04825	0.3336	0.0325	75.2042	-40.23083	-80.128205
	45	186.86940	0.20040	172.69378	0.2086	0.0200	92.3269	-47.5622	-106.269926
	90	193.72776	0.21936	221.70552	0.3196	0.0198	82.0131	-39.4635	-97.465887
2024	0	509.68353	0.11664	738.51396	0.2903	0.0381	359.1992	-102.7798	-52.246604
	45	536.62906	0.10141	607.49868	0.1908	0.0448	371.6999	-86.9649	-93.196645
	90	471.11448	0.09341	662.38702	0.2497	0.0390	344.9915	-88.0426	-97.465887
7075	0	689.57123	0.09233	944.80636	0.2915	0.0811	541.1240	-139.2199	-41.580042
	45	668.14820	0.12595	1001.45578	0.3863	0.0804	484.8701	-136.1382	-33.211558
	90	704.02228	0.08763	1034.37225	0.3178	0.0813	554.3381	-137.1514	-46.576619

According to the **Table 1**, Note that for the same alloy the work hardening coefficient n_H does not have the same value in all directions in the plane of the sheet, for example n_H(0°) = 0.09233, n_H(0°) = 0.08763 and 0.12595 in the direction of 45°for the 7075 alloy. Indeed, for anisotropic materials the two parameters $n_H$and Lankford coefficient depend on the direction in the plane sheet metal [14].

The work hardening coefficient n_H the greater for the 1050 alloy series than the other two series and implies that the 1050 is the most formable.

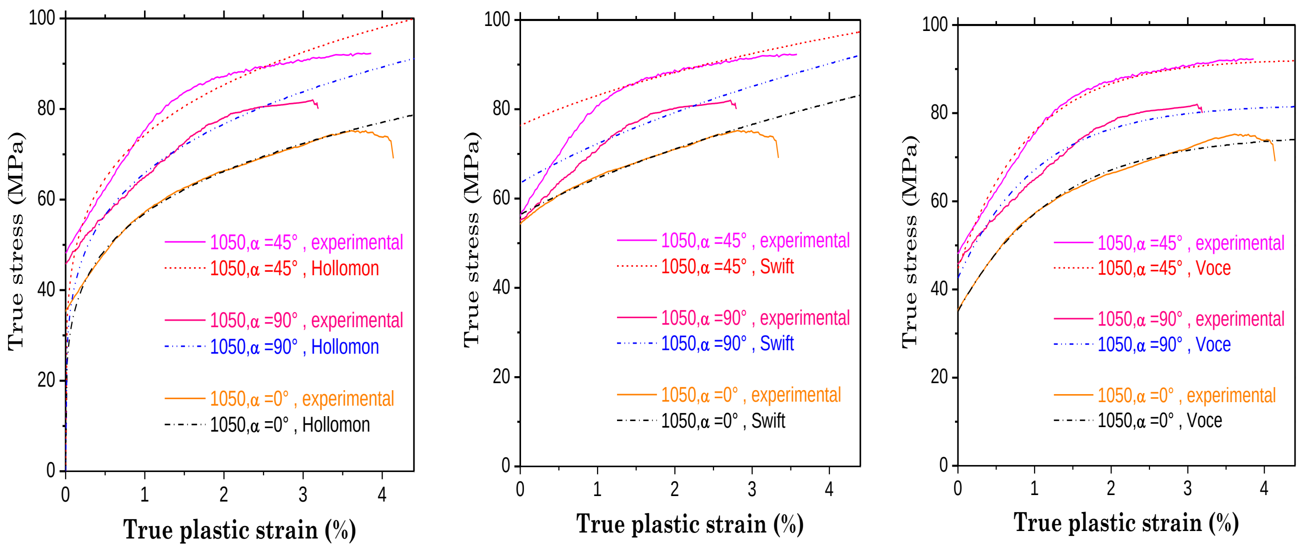

Figure 3 Experimental and theoretical plastic stress-strain curves according to the laws of Hollomon, Swift and Voce of the 1050 serie alloy in the received condition.

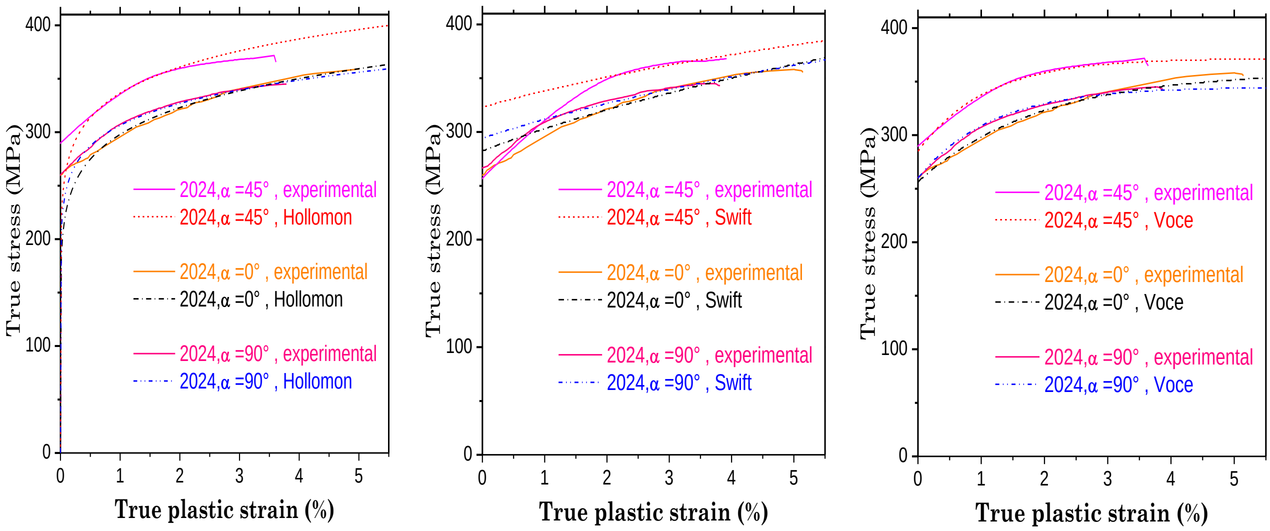

Figure 4 Experimental and theoretical plastic stress-strain curves according to the laws of Hollomon, Swift and Voce of the 2024 serie alloy in the received condition.

According to **Figure 3** we find that Swift's law is the best for describing work hardening, then Hollomon's law, on the other hand Voce's law is the least appropriate among these models.

From **Figure4** we notice that Voce's law describes the work hardening of the 2024 series alloy as much as possible, and that Hollomon's law is the worse one for this alloy.

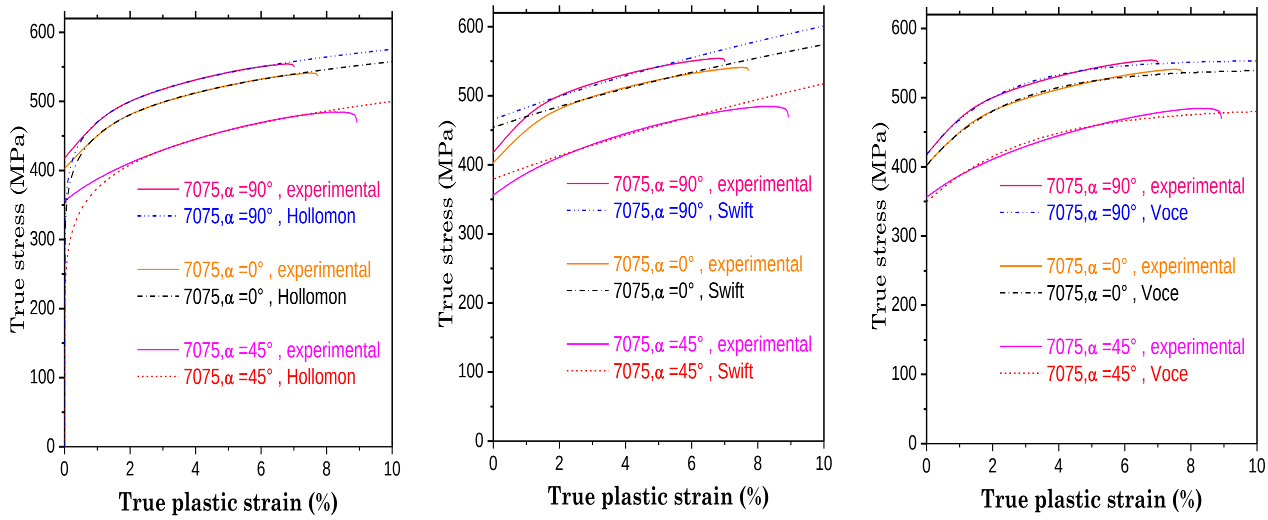

Figure 5 Experimental and theoretical plastic stress-strain curves according to the laws of Hollomon, Swift and Voce of the 7075 serie alloy in the received condition.

From **Figure 5**, it is clear that 7075 serie alloy is easily described by the Hollomon and Swift plastic constitutive laws. Compared to 2024, there are several hardening zones.

6. CONCLUSION

- The experimental results made it possible to study the mechanical properties as well as the identification of the hardening model of each alloy.
- The work hardening laws studied, Hollomon, Swift and Voce are sufficient to describe the plastic behavior of the aluminum alloys studied.

- Hollomon hardening law can describe the plastic behavior for the three alloys studied; however, it is perfect for the 7075 series alloy.
- The best model depends on the alloy studied, not on the directions.
- These identification strategies used in this work can be applied on other materials, this is the goal of the next work.

ACKNOWLEDGEMENTS

I would emphasize the help that I had from the Laboratory of physics of materials (LPM) of the University Sciences and technology Houari-Boumédiène (USTHB), Bab Ezzouar Algeria, where I carried out my present experimental studies in the course of this work.

REFERENCES

[1] STARKE, E. A., STALEY, J. T. Application of modern aluminum alloys to aircraft. *Progress in Aerospace Science*. 1996, vol. 32, no. 2-3, pp. 131-172. Available from: https://doi.org/10.1016/0376-0421(95)00004-6.

[2] SURAPPA, M.K. Aluminium matrix composites: Challenges and opportunities. *Sadhana*. February/April 2003 vol. 28, parts 1 & 2, pp. 319-334.

[3] LAKSHMIPATHY, K.J., KULENDRAN, B. Reciprocating wear behavior of 7075Al/SiC in comparison with 6061Al/Al2O3 composites. *International Journal of Refractory Metals and Hard Materials*. 2014, vol. 46, pp. 137-144.

[4] WITKOWSKA, M., THOMPSON, G. E., HASHIMOTO, T., KOROLEVA, E. Assessment of the surface reactivity of AA1050 aluminium alloy. *Surface and Interface Analysis*. 2013, vol. 45, no. 10, pp. 1585-1589. Available from: https://doi.org/10.1002/sia.5271.

[5] ZEREN, M. Effect of copper and silicon content on mechanical properties in Al-Cu-Si-Mg alloys. *Journal of Materials Processing Technology*. 2005, vol. 169, no. 2, pp. 292-298. Available from: https://doi.org/10.1016/j.jmatprotec.2005.03.009.

[6] KILAAS, R., RADMILOVIC, V. Structure determination and structure refinement of Al2CuMg precipitates by quantitative high-resolution electron microscopy. *Ultramicroscopy*. 2001, vol. 88, pp. 63-72.

[7] RAJAKUMAR, S., MURALIDHARAN, C., BALASUBRAMANIAN, V. Influence of friction stir welding process and tool parameters on strength properties of AA7075-T6 aluminium alloy joints. *Materials & Design*. 2011, vol. 32, pp. 535-549.

[8] SIVARAJ, P., KANAGARAJAN, D., BALASUBRAMANIAN, V. Effect of post weld heat treatment on tensile properties and microstructure characteristics of friction stir welded armour grade AA7075-T651 aluminium alloy. *Defence Technology*. 2014, vol. 10, pp. 1-8.

[9] SMITH, B. The Boeing 777: the development of the Boeing 777 was made possible by the development of breakthrough materials that allowed reductions in structural weight while maintaining affordability. *Advanced Materials & Processes.* Sept. 2003, vol. 161, no. 9, p. 41.

[10] HOLLOMON, J.H. Tensile deformation. *Transactions of the Metallurgical Society of AIME.* 1945, vol. 162, pp. 268-290.

[11] SWIFT, H. W. Plastic instability under plane stress. *Journal of the Mechanics and Physics of Solids*. 1952, vol. 1, no. 1, pp. 1-18. Available from: https://doi.org/10.1016/0022-5096(52)90002-1.

[12] VOCE, E. The relationship between stress and strain for homogeneous deformations. *Journal of the Institute of Metals*. 1948, vol. 74, pp. 537-562.

[13] SIVAPRASAD, P.V., VENUGOPAL, S., VENKADESAN, S. Tensile flow and work-hardening behavior of a Ti-modified austenitic stainless steel. *Metall. Mater. Trans*. A.1997, vol. 28, pp. 171-178. Available from: https://doi.org/10.1007/s11661-997-0092-8.

[14] BOUMAIZA, A. Influence of structural anisotropy of the plastic behavior during deformation by stamping. Constantine, 2008. Ph.D thesis of sciences, University of Mentouri Brothers.